FILME SUBȚIRI TRANSPARENTE CONDUCTOARE CODOPATE CU Al ŞI In DEPUSE PRIN PULVERIZARE CU PIROLIZĂ
TRANSPARENT CONDUCTING Al AND In CODOPED THIN FILM DEPOSITED BY SPRAY PYROLYSIS

A. HADRI[1], B. FARES[1], A. AMARI[1], M. TAIBI[2] ,A. MZERD[1]*
[1]*University Mohammed V- Rabat, Faculty of Sciences, Physics Department, LPM, B.P. 1014, Agdal-Rabat, Morocco.*
[2]*University of Mohammed V, Ecole Normale Superieure,LPCMIN, Rabat-Morocco*

Transparent conducting Al-In codoped ZnO thin films were successfully synthesized onto glass substrates by spray pyrolysis technique. The influence of doping and codoping on the structural, optical and electrical properties was investigated. X-ray diffraction results showed that the samples have the hexagonal Würtzite structure with a preferred orientation toward the c-axis. No peaks belonging to In and Al or their oxides was observed in the limit of XRD technique detection. EDS analysis confirmed the presence of In and Al elements in ZnO thin films. The atomic percentage of In and Al elements was nearly equal to their nominal stoichiometry. The surface morphology of the codoped films showed well-defined hexagonal grains. Examination through transmission electron microscopy depicted that these films consists of an agglomeration of small grains with hexagonal shape. A high transmittance above 75% and electrical resistivity around 3×10^{-2} Ω.cm were reached after annealing.

Keywords: *Spray pyrolysis, Hall Effect, ZnO, aluminum-indium codoped ZnO.*

1. Introduction

Among various transparent conducting oxides (TCO), zinc oxide (ZnO) has been received more and more attention. It holds an important position in the field of material science due to its wide band gap, large exciton binding energy (60 meV) and high stability in hydrogen plasma [1-4]. These unique properties make ZnO extensively used in a wide range of applications such as transistors [5], solar cells and sensors [6-7]. Recently, several physical and chemical methods have been employed to prepare ZnO thin films such as magnetron sputtering [8], pulsed laser deposition [9], chemical vapor deposition [10], spray pyrolysis [11], sol-gel [12]. Generally, physical techniques are commonly used; however the cost is relatively high. In the present investigation we will focus on the spray pyrolysis technique due to its cost effectiveness as it does not require sophisticated vacuum apparatus and well adapted for mass fabrication.

The electrical conductivity of undoped ZnO is relatively low, which cannot meet the demands of several application fields. To improve electrical, optical and other properties of ZnO, It is practical to dope ZnO with group III elements [13-15]. In single doped ZnO, Al doped ZnO (AZO) have attracted most of the researchers' attention due to its numerous advantages in terms of conductivity and chemical stability [16-18], while others choose In as dopant (IZO) due to its lower reactivity and greater resistivity to oxidation [19-20]. Furthermore, studies emphasized that codoping with low concentration in ZnO films can optimize their physical properties. For example, Al-V codoped ZnO and Al-Y codoped ZnO thin films have showed an improved thermal stability and electrical conductivity, respectively [21-22]. Therefore, it appears that Al and In codoped ZnO (IAZO) can be attractive.

In this paper, undoped ZnO,IZO and IAZO thin film were synthesized on glass substrates by spray pyrolysis method and the structure, electrical and optical properties of these films were studied and discussed.

2. Experimental details

Undoped ZnO, IZO and IAZO thin films were successfully synthesized on glass substrates by spray pyrolysis technique using different Al content. A homogenous solution were prepared by dissolving zinc chloride $ZnCl_2$, Indium Chloride $InCl_3$ and aluminum nitrate nona-hydrate ($Al(NO_3)_3,9H_2O$) in 200 mL of distilled water in order to prepare the starting solution with a concentration of 0.05M. Undoped ZnO and IZO were used as a reference samples. The Al content was varied at 0 at.%, 1 at.% and 2 at.%, while In content was fixed at 3 at.%, and were named IZO3, IAZO1 and IAZO2 respectively. The content of Al and In in the starting solution is referred here as the

* Autor corespondent/*Corresponding author,*
E-mail: mzerd@yahoo.fr

atomic percentage with respect to Zn. The detailed description of experimental procedure has been given elsewhere [20]. The as deposited IZO3, IAZO1 and IAZO2 were annealed in tubular furnace at 350 °C for 2h in argon atmosphere.

The deposited films were characterized in order to study their chemical and physical properties. X-ray diffraction (XRD, Siemens D 5000) was carried out, using Cu-kα radiation, λ=1.5405Å, to analyze the crystallite size and growth orientation of the as-deposited films. The In/metal and Al/metal composition of the films on glass substrates were investigated by energy dispersive spectroscopy (EDS). The surface morphology and topography were examined by Scanning Electron Microscopy (SEM, FEI Quanta 200) and Atomic Force Microscopy (AFM), operating in tapping mode. Transmission electron microscope (TEM) micrographs were obtained using Topcon 002b. Electrical properties of the films have been performed by Ecopia HMS 3000 Hall effect measurements system using the four probes Van der Pauw configuration. The measurements have been done at room temperature and the ohmic behavior of the contacts has been confirmed prior to Hall measurements. The Hall measurements have been repeated several times for each sample to confirm the consistency of our results. The optical transmittance spectra were obtained using UV-visible spectrophotometer (PerKilmer Lambda 900) and taking into account the glass in the reference beam.

3. Results and discussion

3.1. Structure and surface morphology

To investigate the effect of doping and codoping on the microstructure of the elaborated thin films, XRD analysis was performed. Figure 1 illustrates the XRD patterns of undoped ZnO, IZO and IAZO thin films.

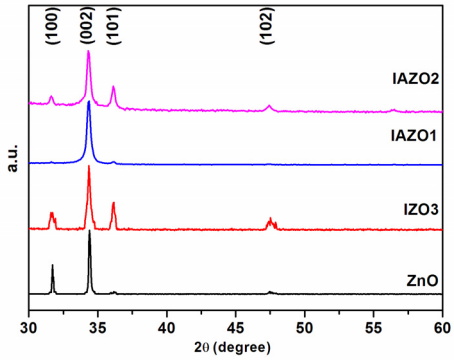

Fig. 1 - X-ray diffraction spectra of the deposited thin films.

As seen from this figure, four diffraction peaks are observed which are related to (100), (002), (101) and (102) orientations [JCPDS-card No 89-1397], indicating a polycrystalline structure that belonged to the ZnO würtzite structure. The absence of other peaks even for the film deposited with highest Al content in the starting solution precludes the possibility of any extra phases related to Al or In in the films (within the sensitivity limitation of XRD). In all cases, the other peaks are lower in comparison with (002) peak suggesting that the crystalline structure of the films is mainly oriented with their c-axis perpendicular to the substrate irrespective of the doping content. Moreover, the (002) diffraction peak is the sharpest when the Al content is 1at.%, which implied that the impurities were stabilized in the IAZO1 structure system. L. Balakrishnan et al. confirmed that the high intensity of (002) peak was attributed to the improvement of stoichiometry by optimum incorporation of dopant atoms [23].

The texture coefficient [24] (TC) of the (002) plane was calculated and listed in Table1. It is seen that all the thin films have a (002) preferential orientation and that the codoped films with the lowest Al content shows the highest value. This could be attributed to the small ionic radius of aluminum compared to that of zinc and indium, which at lower concentration occupy mainly substitution sites and therefore change the growth pattern. As the Al content increases above 1%, the texture coefficient decreases which may be due to the limited solubility of Aluminum. As a consequence, the aluminum excess may occupy interstitial sites that affect the cystallinity of the films.

Table 1

Structural parameters of ZnO, IZO and IAZO thin films

Samples	D(nm)	$TC_{(002)}$	a (Å)	c (Å)
ZnO	49.1	2.81	3.190	5.210
IZO3	34.6	1.96	3.202	5.230
IAZO1	28.1	3.84	3.197	5.222
IAZO2	29.7	2.96	3.198	5.223

The crystallite size of the films were calculated from the (002) peak in the XRD profile by using Scherrer's formula [25] (see Table 1). The significant decrease in grain size was attributed to the fact that some of the doping atoms prefer to locate in the grain boundary regions and inhibit the grain growth due to the difference of atomic radius of zinc and doping elements (In, Al).

The lattice constant (a) and (c) were obtained using the inter-reticular distance d_{hkl} of the hexagonal structure and are found to be in good agreement with the usually published values of ZnO [26, 27]. Compared to the undoped ZnO film, the increase in the lattice constant observed in IZO3 thin film was attributed to the difference in

the ionic radii of zinc and indium (R_{Zn2+}=0.074 nm and R_{In3+}=0.08 nm). On the other hand, the lattice parameter of the codoped film exhibits two behaviors. At low aluminum content (1 at.%), the lattice parameter first decreased which was due to the substitution of Zn^{2+} ions by Al^{3+} (0.053 nm) which contribute in the size compensation between Al^{3+} and In^{3+} in ZnO lattice. However, increasing Al content above 1at.%, leads to a slight increase of the lattice parameter as compared with IAZO1, which is probably due to the introduction of Al ions in the interstitial sites [28]. These observations have been well supported by our Hall Effect measurement results.

The local chemical compositions of the doped and codoped thin films were characterized by EDS. Table 2 summarizes the atomic percentage of the elemental composition data derived from the main constituents; Zn, O, In and Al in IZO and IAZO thin films respectively. It clearly confirms the presence of In and Al elements in codoped thin films and shows that the intensity of Al elements increases with increasing Al doping content. The values of the atomic percentages of In/metal ion ratio and Al/metal ion ratio are close to their nominal stoichiometry and thus allowing us to study the effect of increasing Al content in the codoped films. Taking in account the XRD results, it can be concluded that In and Al ions are successfully incorporated into the ZnO structure without changing the phase.

The morphology, topography and structural characterization of the thin films were analyzed using SEM, AFM and TEM. Figure 2 shows SEM images of the deposited films. All films indicate an uniform morphology, however, the films are found to be dependent on doping content. As it can be seen the Al doping content exhibits a noticeable influence on the surface morphology of IAZO thin films. The surface of IZO3 thin films exhibits a pyramid shape. When the Al content increases, the surface of IAZO thin films evolves towards nearly hexagonal shape. The grain sizes of the codoped films were estimated to be 547 and 1200 nm for IAZO1 and IAZO2, respectively. These grain sizes are higher than that calculated from the X-ray that may be attributed to the agglomeration of the indium metal on the IAZO thin films, indicating that these grains are formed by several crystallites [29].

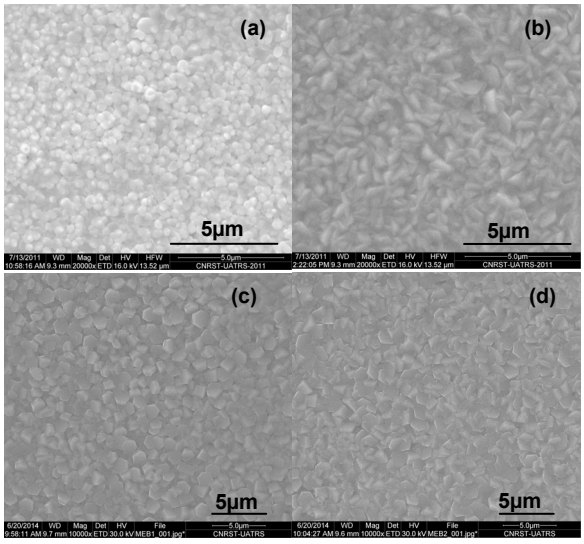

Fig. 2 - SEM images of ZnO (a), IZO3 (b), IAZO1 (c) and IAZO2 (d) thin films.

The three dimensional (3D) of different sized AFM micrographs were presented in Figure 3. The prepared films show various topography of surface grains, which are dependent on the doping element. The 3D images exhibit separated conical columnar microstructure of various hight in the undoped film which is characteristic of the common metal oxide as reported by M. Benhaliliba et al. [30], whereareas coalescence of some columnar grains are seen in the IZO fillms.

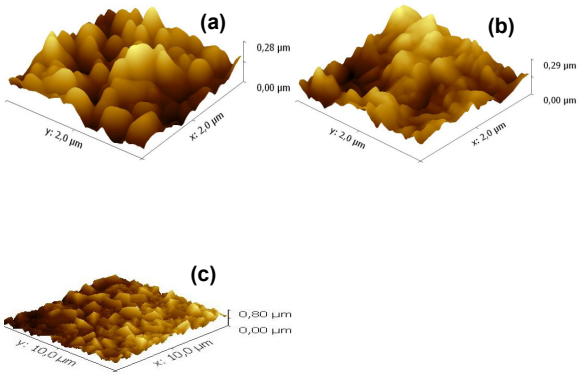

Fig. 3 - 3D AFM images of (a) undoped ZnO, (b) IZO3, (c) IAZO1.

Table 2

Chemical composition of IZO and IAZO thin films

Samples	Atomic (%)				In/(Zn+In+Al) (%)	Al/(Zn+Al+In) (%)
	Zn	O	In	Al		
IZO3	75.9	21.9	2.1	-	2.8	-
IAZO1	63.1	34.3	1.9	0.8	2.8	1.2
IAZO2	67.7	29.4	1.8	1.2	2.5	1.7

On the other hand, the films surface of IAZO1consist of some sharply pointed grains stacked in certain favorable sites. In addition, it can be seen from the micrographs a few black patches in the inner region between stacked grain which correspond to certain non favorable sites and represent few voids on the film surface. These observations are in good agreement with XRD pattern analysis and confirm that the grains are oriented along the c-axis.

Since the XRD gives the average crystallite size and SEM gives the size of the agglomerated particles, the accurate size of the particles can be determined from TEM measurements [31]. TEM images of IZO3, IAZO1 and IAZO2 are shown in Figure 4 (a), (b) and (c) respectively. The images reveal that the crystallites have a spherical shape and that small grains coalesced together to form large grains. The estimated values of particle size of codoped films from TEM photographs were varied between 5 and 10 nm.

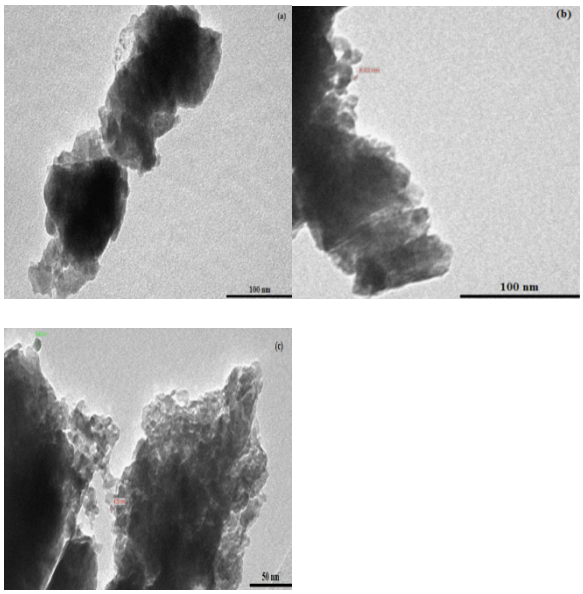

Fig. 4 - TEM images of IZO3 (a), IAZO1 (b) and IAZO2 (c) thin films.

3.2. Electrical Properties

Hall Effect measurements were performed at room temperature to investigate the electrical properties of the deposited films. The results obtained are listed in Table 3. It was observed that the electrical resistivity of the undoped ZnO was the highest, 66 Ω.cm, which is owing to both low carrier concentration and low mobility. However, the electrical resistivity was reduced in the IAZO1 thin film which exhibits the lowest resistivity of 0.1Ω.cm. This result was mainly affected by the carrier concentration. This behavior can be explained by a partial substitution of Zn^{2+} ions by In^{3+} and Al^{3+} ions, where each substitution generates one free electron in the conduction band, which eventually increased the carrier concentration. In contrast, further increase of Al content lead to a deterioration of the electrical properties. As a result, the carrier concentration decreases, which is mainly due to the excess of Al atoms which as stated before segregates in interstitial positions and disturb the generation of free electron.

Conventionally, the Hall mobility is controlled by carrier scattering. The Hall mobility fluctuated with varying the amount of doping elements. To explore the effects of doping and codoping on the Hall mobility, the mean free path ℓ [32] was calculated and listed in Table 3. It is known, that the grain boundary scattering is considered as one of the important scattering mechanism in polycrystalline semi-conductor thin film [33]. However, the scattering mechanism by grain boundaries in most cases is negligible if the mean free path of electrons is smaller than the crystallite size [33,34]. As shown in Table 3, all the films present smaller values than the crystallite size. Therefore the impurity scattering is the predominant factor compared with other scattering factors. Furthermore the slight decrease of Hall mobility in the codoped film after increasing Al content to 2 at.% may be attributed to the rise of repulsive interaction between In and Al dopants in interstitial position.

To improve the quality and reduce defects a post annealing treatment was performed. The electrical properties of annealed IZO3, IAZO1 and IAZO2 are listed in Table 3. After annealing the resistivity of IAZO films became lowered due to the increase carrier concentration. The codoped film with the lowest resistivity of 3×10^{-2} Ω.cm was obtained for IAZO1 films. The observed increase in carrier concentration or/and Hall mobility of IAZO films can be related to the ionization of oxygen vacancies and by desorption of oxygen in the grain boundaries which acts as traps for carriers [35].

Table 3

Electrical parameters of ZnO, IZO and IAZO thin films.

Samples	ρ ($\times10^{-1}$ Ω.cm)	n ($\times10^{18}$ cm^{-3})	μ ($cm^2.V^{-1}.s^{-1}$)	ℓ Mean free path (nm)
ZnO (as deposited)	660.0	0.3	0.3	0.001
IZO3 (as deposited)	3.0	0.5	46.2	0.7
IZO3 (annealed)	0.2	570	0.6	0.1
IAZO1 (as deposited)	1.1	46	1.21	0.08
IAZO1 (annealed)	0.3	590	0.3	0.05
IAZO2(as deposited)	5.1	24	0.5	0.02
IAZO2 (annealed)	0.5	119	1.03	0.1

Table 4
Electrical resistivity of trivalents elements codoped ZnO thin films as reported by other authors and in present work

Preparation technique and precursors	Co-doping elements	Annealing treatment	ρ (×10^{-2} Ω cm)	references
Spray pyrolysis (350 °C, $ZnCl_2$, Al $(NO)_3$ $9H_2O$, $InCl_3$)	(Al^{3+}, In^{3}+)	(350 °C, Argon atmosphere)	3	This work
Spray pyrolysis (350 °C, $Zn(CH_3COO)_2$, $2H_2O$, $YbCl_3$ $6H_2O$, TmCl3 6H2O).	(Yb^{3+}, Tm^{3+})	-	5.7	[37]
Sputtering	(Al^{3+}, $Ga^{3+)}$	(600 °C, H_2 ambient)	0.1	[38]
RF-DC Sputtering	(Al^{3+}, Sc^{3+})	(300°C, Ar-atmosphere)	48	[39]
Sol–Gel spin-coating (100 °C,$In(NO_3)_3$, $Zn(NO_3)_2$, $Y(NO_3)\cdot 4H_2O$)	(In^{3+}, Y^{3+})	(500 ◦C, dry air atmospheres)	700	[40]
Sol-Gel (300 °C, $Zn(CH_3COO)_2\cdot 2H_2O$, $Al(NO_3)_3\cdot 9H_2O$, $Ga(NO_3)_3\cdot 9H_2O$)	(Al^{3+}, Ga^{3+})	(500 °C)	□ 500	[41]

However, the mobility of the annealed IZO3 and IAZO1 films decreased as compared with the as deposited films, which may be attributed to ionized impurity scattering since the mobility of highly degenerated semi-conductor is known to be disproportional to carrier concentration $\mu \alpha \eta^{-2/3}$ [36]. One can note that codoping of ZnO with Al and In via spray pyrolysis method and annealing can improve the electrical resistivity of the films. Furthermore, Table 4 summarizes the comparison of the lowest resistivity obtained after annealing in this work with those reported in literature [37 - 41]. As it can be seen, our results are comparable to those obtained using more sophisticated and expensive technique such as sputtering.

3.3. Optical properties

Figure 5 presents the UV-Vis transmittance spectra of ZnO, IZO and IAZO thin films in the wavelength interval of 350-800 nm (a) and comparison between annealed and as-deposited IZO and IAZO1 thin films (b). All the films showed a sharp fundamental absorption around 375 nm with a high average transmittance (over than 80% in the visible region). However, the transmittance of the doped and codoped film slightly decreased as compared with undoped ZnO. This tendency may be due to the higher carrier concentration in those films. Moreover, the absence of the interference fringes in the transmittance spectra is attributed to the diffusion phenomena due to the small grain size. After annealing, it is seen that the average transmittance in the visible region of the selected films decreased slightly but remains above 76%. This observation can be related to the carrier concentration in both films. In addition, the low transmittance of IAZO1 as compared to IZO3 films may be attributed to the increase of active metal element which affects the optical transmittance.

4. Conclusion

The transparent conducting ZnO, IZO and IAZO thin films were successfully prepared on glass substrates by spray pyrolysis. The structural, electrical and optical properties of the films with various Al content were mainly investigated in this work. All the films showed a preferential orientation along (002) direction, and the diffraction peak was enhanced with increasing Al content to 1at.%. In addition, the doping and codoping content alters the morphology and grain size of the samples. Moreover, TEM images showed an agglomerated grains which were attributed to Indium doping. The lowest resistivity, 1.1×10^{-1} Ω.cm, was obtained for the sample codoped with 1% Al content which combined with a high transmittance, above 80%, in the visible range. The electrical properties of this film were further improved after annealing process and a resistivity of 3×10^{-2} Ω.cm was achieved. The

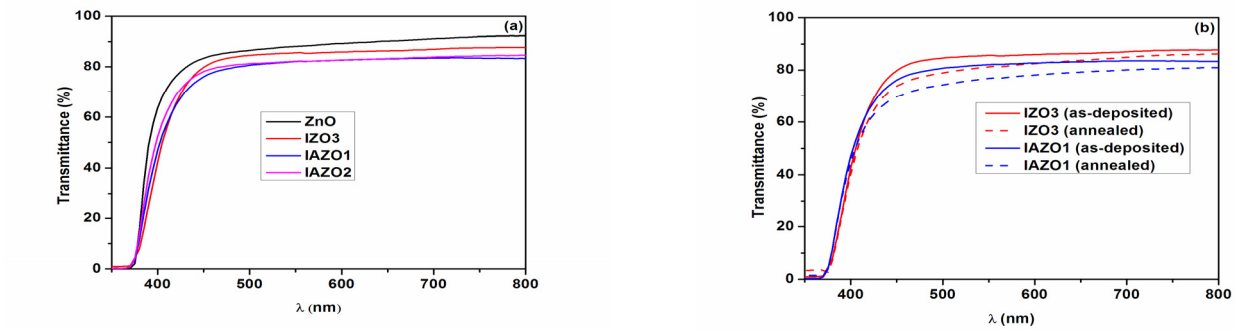

Fig. 5 - UV-Vis transmittance spectra of ZnO, IZO and IAZO thin films (a) and comparison between as-deposited and annealed IZO, IAZO1 thin films (b).

obtained results suggest that the control of Al codoping amount plays an important role in growing a high quality films.

Acknowledgments

The authors are thankful to Professor A. BELAYACHI, member at the Laboratory of Materials and Science at Rabat. This work was supported by the University of Mohammed V- Rabat.

REFERENCES

1. J. C. Fan, K. M. Sreekanth, Z. Xie, S. L. Chang and K. V. Rao, p-Type ZnO materials: Theory, growth, properties and devices, Progress in Materials ***Science,*** 2013, **58**, 874.
2. A. B. Djurisic, X. Y. Chen, Y. H. Leung and A. M. C. Ng, ZnO nanostructures: growth, properties and applications, Journal of Materials Chemistry, 2012, **22**, 6526.
3. J. Gupta, K. C. Barick and D. Bahadur, Defect mediated photocatalytic activity in shape-controlled ZnO nanostructures, Journal of Alloys and Compounds, 2011, **509**, 6725.
4. Z. Pan, P. Zhang, X. Tian, G. Cheng, Y. Xie, H. Zhang, X. Zeng, C. Xiao, G. Hu and Z. Wei, Properties of fluorine and tin co-doped ZnO thin films deposited by sol–gel method, Journal of Alloys and Compounds, 2013, **576**, 31.
5. S. N. Cha, J. E. Jang, Y. Choi, G. A. J. Amaratunga, G.W. Ho, M. E. Welland, D. G. Hasko, D. J. Kang and J. M. Kim, High performance ZnO nanowire field effect transistor using self aligned nanogap gate electrodes, Applied Physics Letters, 2006, **89**, 263102.
6. K. Djessas, I. Bouchama, J. L. Gauffier and Z. Ben Ayadi, Effects of indium concentration on the properties of In-doped ZnO films: Applications to silicon wafer solar cells, Thin Solid Films, 2014, **555**, 28.
7. T. Santhaveesuk and S. Choopun, Ethanol sensing characteristics of Sn-doped ZnO tetrapods, Sensor Advanced Materials Research, 2013, **770**, 185.
8. J. W. Lee, K. N. Hui, K. S. Hui, Y. R. Cho and H. H. Chun, Low resistivity of Ni–Al co-doped ZnO thin films deposited by DC magnetron sputtering at low sputtering power, Applied Surface Science, 2014, **293**, 55.
9. A. Taabouche, A. Bouabellou, F. Kermiche, F. Hanini, Y. Bouachiba, A. Grid and T. Kerdjac, Properties of cobalt-doped zinc oxide thin films grown by pulsed laser deposition on glass substrates, Materials Science in Semiconductor Processing, 2014, **28**, 54.
10. X. H. Wang, L. Q. Huang, L. J. Niu, R. B. Li, D. H. Fan, F. B. Zhang, Z. W. Chen, X. Wang and Q. X. Guo, The impacts of growth temperature on morphologies, compositions and optical properties of Mg-doped ZnO nanomaterials by chemical vapor deposition, Journal of Alloys and Compounds, 2015, **622**, 440.
11. A. Hadri, C. Nassiri, F. Z. Chafi, M. Loghmarti, B. Fares, L. Laanab, F. Chraibi, M. Bensitel and A. Mzerd, Indium Doping Effect on Structural, Optical and Electrical Properties of Sprayed ZnO Thin Films, Sensors & Transducers, 2014, **178**, 63.
12. X. Liu, K. Pan, W. Li, D. Hu, S. Liu and Y. Wang, Optical and gas sensing properties of Al-doped ZnO transparent conducting films prepared by sol–gel method under different heat treatments, Ceramics International, 2014, **40**, 9931.
13. J. Y. Cho, S. W. Shin, Y. B. Kwon, H. K. Lee, K. U. Sim, H. S. Kim, J. H. Moon and J. H. Kim, Wide band gap characteristic of quaternary and flexible Mg and Ga co-doped ZnO transparent conductive thin films, Thin Solid Films, 2011, **519**, 4282.
14. S. W. Shin, I. Y. Kim, G. H. Lee, G. L. Agawane, A. V. Mohokar, G. S. Heo, J. H. Kim and J. Y. Lee, A study on the epitaxy nature and properties of 3 wt% Ga-doped epitaxial ZnO thin film on Al_2O_3 (0001) substrates, Crystal Growth & Design, 2011, **11**, 4819.
15. S. U. Park and J. H. Koh, Low temperature rf-sputtered In and Al co-doped ZnO thin films deposited on flexible PET substrate, Ceramics International, 2014, **40**, 10021.
16. J. J. Ding, H. X. Chen and S. Y. Ma, The Al-doping and post-annealing treatment effects on the structural and optical properties of ZnO:Al thin films deposited on Si substrate, Applied Surface Science, 2010, **256**, 4304.
17. E. Bacaksiz, S. Aksu, S. Yılmaz, M. Parlak and M. Altunbas, Structural, optical and electrical properties of Al-doped ZnO microrods prepared by spray pyrolysis, Thin Solid Films, 2010, **518**, 4076.
18. Y. H. Kim, K. S. Lee, T. S. Lee, B. Cheong, T. Y. Seong and W. M. Kim, Effects of substrate temperature and Zn addition on the properties of Al-doped ZnO films prepared by magnetron sputtering, Applied Surface Science, 2009, **255**, 7251.
19. G. Singh, S. B. Shrivastava, D. Jain, S. Pandya, T. Shripathi and V. Ganesan, Effect of indium doping on zinc oxide films prepared by chemical spray pyrolysis technique, Bulletin of Materials *Science*, 2010, **33**, 581.
20. A. Hadri, M. Loghmarti, A. Mzerd, M. Taibi, Preparation and characterization of Al doped ZnO thin films by spray pyrolysis, International Renewable and Sustainable Energy Conference (IRSEC), 2014, 61.
21. S. Suzuki, T. Miyata, M. Ishii and T. Minami, Transparent conducting V-co-doped AZO thin films prepared by magnetron sputtering, Thin Solid Films, 2003, **434**, 14.
22. Y. Z. Tsai, N. F. Wang, M. R. Tseng and F. H. Hsu, Transparent conducting Al and Y codoped ZnO thin film deposited by DC sputtering, Materials Chemistry and Physics, 2010, **123**, 300.
23. L. Balakrishnan, S. Gowrishankar and N. Gopalakrishnann, Fabrication of tridoped p-ZnO thin film and homojunction by RF magnetron sputtering, Ceramics International, 2012, **38**, 6221.
24. A. Hadri, C. Nassiri, F. Z. Chafi, M. Loghmarti, and A. Mzerd, Effect of Acetic Acid Adding on Structural, Optical and Electrical Properties of Sprayed ZnO Thin Films, Energy Environ. Focus, 2015, **4**, 12.
25. B.D. Cullity and S.R. Stock, Elements of X-ray Diffraction, edited by Prentice-Hall (Englewood Cliffs, New Jersey, 2001) p. 170.
26. A. Hadri, C. Nassiri, F.Z. Chafi, M. Loghmarti, M. Tricha and A. Mzerd, Characterization Of In-Doped And Ga-Doped Zinc Oxide Film Deposited By Spray Pyrolysis, Physical and Chemical News, 2015, **75**, 1.
27. A. Hadri, M. Taibi, M. loghmarti, C. Nassiri, T. Slimani Tlem□ani, A. Mzerd, Development of transparent conductive indium and fluorine co-doped ZnO thin films: Effect of F concentration and post-annealing temperature, Thin Solid Films, 2015 (In Press).
28. P. Sagar, M. Kumar and R. M. Mehra, Influence of hydrogen incorporation in sol-gel derived aluminum doped ZnO thin films, Thin Solid Films, 2005, **489**, 94.
29. L. Raniero, I. Ferreira, A. Pimentel, A. Gonc- alves, P. Canhola, E. Fortunato and R. Martins, Role of hydrogen plasma on electrical and optical properties of ZGO, ITO and IZO transparent and conductive coatings, Thin solid Films, 2006, **511**, 295.
30. M. Benhaliliba, C. E. Benouis, Z. Mouffak, Y. S. Ocak, A. Tiburcio-Silver, M. S. Aida, A. A. Garcia, A. Tavira and A. Sanchez Juarez, Preparation and characterization of nanostructures of in-doped ZnO films deposited by chemically spray pyrolysis: Effect of substrate temperatures, Superlattices and Microstructures, 2013, **63**, 228.
31. N. Rajamanickam, S. Rajashabala and K. Ramachandran, Theoretical and experimental investigation on enhanced thermal behavior in chunk shaped nano ZnO, *Molecular Physics*, 2014, **12**, 142.
32. K. H. Ri, Y. B. Wang, W. L. Zhou, J. X. Gao, X. J. Wang and J. Yu, The structural properties of Al doped ZnO films depending on the thickness and their effect on the electrical properties, Applied Surface Science, 2011, **258**, 1283.
33. Z. Y. Zhang, C. G. Bao, W. J. Yao, S. Q. Ma, L. L. Zhang and S. Z. Hou, Influence of deposition temperature on the crystallinity of Al-doped ZnO thin films at glass substrates prepared by RF magnetron sputtering method, Superlattices and Microstructures, 2011, **49**, 644.

34. B. Houng and H.B. Chen, Investigation of AlF3 doped ZnO thin films prepared by RF magnetron sputtering, Ceramics International, 2012, **38**, 801.
35. D. K. Kim and H. B. Kim, The reason of degradation in electrical properties of ZnO:Al thin films annealed with various post-annealing temperature, Current Applied Physics, 2013, **13**, 2001.
36. M. Chen, Z. L. Pei, X. Wang, Y. H. Yu, C. Sun and L. S. Wen, Intrinsic limit of electrical properties of transparent conductive oxide films, Journal of Physics D: Applied Physics, 2000, **33**, 2538.
37. I. Chaki, A. Belayachi, T. El Bahraoui, M. Regragui and M. Abd-Lefdil, Semiconducting properties of Tm doped Yb-ZnO films by spray pyrolysis, European Physical Journal Applied Physics, 2014, **68**, 30301.
38. K. W. Seo, H. S. Shin, J. H. Lee, K. B. Chung and H. K. Kim, The effects of thickness on the electrical, optical, structural and morphological properties of Al and Ga co-doped ZnO films grown by linear facing target sputtering, Vacuum, 2014, **101**, 250.
39. J. C. Lin, K. C. Peng, H. L. Liao and S. L. Lee, Transparent conducting Sc-codoped AZO film prepared from ZnO:Al–Sc by RF-DC sputtering, Thin Solid Films, 2008, **516**, 5349.
40. C. C. Ting, S. P. Chang, W. Y. Li and C. H. Wang, Enhanced performance of indium zinc oxide thin film transistor by yttrium doping, Applied Surface Science, 2013, **284**, 397.
41. R. Ebrahimifard, M. R. Golobostanfard, H. Abdizadeh, Sol–gel derived Al and Ga co-doped ZnO thin films: An optoelectronic study, Applied Surface Science, 2014, **290**, 252.

****

MANIFESTĂRI ŞTIINȚIFICE / SCIENTIFIC EVENTS

The International Conference on Technological Advances of Thin Films & Surface Coatings is a biennial event of knowledge exchange and interactive platform for researchers and engineers from industry, research laboratories and academia. ThinFilms2016 is the 8th of this series.

- Biological Coatings (BCT)
- Coatings for Clean Energy (CCE)
- Coating towards Industrial Applications (CIA)
- Electrochemistry and Corrosion of Thin Films (ECF)
- Functional Thin Films for Energy Photonics (FEP)
- Ion-conducting thin films (ICF)
- Mechanical Properties of Thin Films (MPF)
- Nanostructured and Nanocomposite Films and Coatings (NNF)
- Optoelectronic and Dielectric Thin Films (ODF)
- Oxide Thin Films, Nano- & Heterostructures (OFN)
- Organic/Polymer Thin Films (OPF)
- Optical Thin Films (OTF)
- Smart Materials and Films (SMF)

Contact: http://www.thinfilms.sg/conferences/thinfilms-2016

****